JOURNAL OF CATALYSIS **159,** 236–245 (1996)
ARTICLE NO. 0083

Hydrodesulfurization of Methyl-Substituted Dibenzothiophenes: Fundamental Study of Routes to Deep Desulfurization

M. V. Landau,[1] D. Berger, and M. Herskowitz

Blechner Research Center for Industrial Catalysis and Process Development, Ben-Gurion University of the Negev, Beer-Sheva, Israel 84105

Received June 30,1995; revised September 26, 1995; accepted October 13, 1995

Four catalysts, Co–Mo and Ni–Mo, designed to cover a wide range of activity for aromatic ring hydrogenation and two catalysts, zeolite-Co–Mo, with different cracking activities were tested, in the hydrodesulfurization of dibenzothiophene (DBT) and 4,6-dimethyl-DBT (DMDBT) in a fixed-bed reactor at 360°C and a hydrogen pressure of 5.4 MPa. Increasing the hydrogenation activity of the catalysts increased the mole ratio, α, of cyclohexylbenzenes to biphenyls produced from both reactants. Although α had little effect on the hydrodesulfurization (HDS) rate of DBT, the HDS rate of DMDBT increased significantly with α, approching the same level as for DBT at α=2. Introduction of zeolite H-ZSM-5 to the Co–Mo –Al catalyst increased the HDS rate of DBT at a lower value of α and decreased that of DMDBT. No cracking reactions of DBT and DMDBT were detected. A Co–Mo–Al catalyst containing HY zeolite displayed significant cracking activity of DMDBT defined by two routes: demethylation of benzenic rings and scission of the C–C bond connecting the benzenic rings. It resulted in increasing HDS rates of DMDBT by about threefold relative to the Co–Mo–Al catalyst, yielding toluene and benzene, at a ratio of about 3, as the main HDS products. About 80% of the DMDBT desulfurized with HY–Co–Mo–Al catalyst was converted through "cracking" intermediates, 90% of those intermediates being produced through the scission of the C–C bond connecting the benzenic rings. © 1996 Academic Press, Inc.

INTRODUCTION

A growing interest in the deep desulfurization of diesel fuels has been recorded as a result of new regulations designed to limit the sulfur content to 0.05 wt% (1, 2). 4-Methyldibenzothiophene (4-MeDBT) and 4,6-dimethyldibenzothiophene (DMDBT) were reported to react at a low rate in the deep hydrodesulfurization (HDS) of middle distillate feedstocks such as light oil (3–5). Their HDS rates on standard Co–Mo–Al hydrodesulfurization catalysts are lower by a factor of 10–15 compared with dibenzothiophene (DBT) (6, 7) which translates into high temperatures (more than 380°C) for this process (5). Current Co(Ni)–Mo–Al commercial catalysts for HDS of atmospheric gas oils remove the DBT sulfur at normal operating conditions in hydrodesulfurizers (350–360°C) (5–8). Deep desulfurization requires new catalytic routes for efficient desulfurization of methylated DBT.

It has been proved (9) that methyl substituents in the 4- and 6-positions of DBT increase its chemisorption through the π electrons of the aromatic rings in flat mode parallel to the catalyst surface. It was supposed (9) that they hinder sterically the DBT adsorption on the catalyst surface by a sulfur-bonded mode preventing the C–S bond scission. However, according to theoretical calculations (10) both DBT and methylated DBT adsorb flat on the catalyst surface. Hence the decrease in reactivity of the DBT molecule in the presence of methyl groups in the 4- and 6-positions could be a result of hindering the access of hydrogen to the C–S–C bridge after flat adsorption. Potential catalytic routes that involve some intermediate transformations like hydrogenation of benzenic rings, demethylation, scission of the single C–C bond in the thiophenic ring, and isomerization of methyl groups from 4,6- to 1,9-positions could activate the methylated DBT.

Several studies have been published recently in this field. Kabe *et al.* measured the product distribution in HDS of DBT, 4-Me-DBT, and 4,6-DMDBT with a Co–Mo–Al catalyst (9). They found that the desulfurization route by intermediate hydrogenation of the aromatic ring was not inhibited by addition of methyl substituents to DBT. However, only 10–15% of desulfurized methylated DBT was converted through the hydrogenation route, probably because of a low hydrogenation activity of the catalyst. Takaaki *et al.* (11) reported that, using a sulfided Co–Mo–Al catalyst, the contribution of the hydrogenation route in the HDS of DMDBT, 4-Me-DBT, and DBT was 94, 37, and 12%, respectively. That could be the reason for the higher activity of Ni–Mo–Al compared with Co–Mo–Al in the HDS of methylated DBT reported by Ma *et al.* (7). However, there is still no evidence that increasing the catalyst hydrogenation activity accelerates the DMDBT HDS. Other routes, intermediate isomerization of substituted DBT and demethylation as a result of reaction with polyaromatic molecules, catalyzed by zeolites Y and ZSM-5, were tested

[1] To whom correspondence should be addressed.

0021-9517/96 $18.00
Copyright © 1996 by Academic Press, Inc.
All rights of reproduction in any form reserved.

by Rollmann *et al.* (12). No information was given about the effectiveness of those routes in HDS of methyl-substituted DBT.

The purpose of this study is to investigate two routes for desulfurization, intermediate hydrogenation and cracking of DMDBT, to enhance the rate of the HDS reaction.

METHODS

Catalyst Preparation and Characterization

Six catalysts were used in this study, commercial Co–Mo–Al (I) and Ni–Mo–Al (II) and four proprietary catalysts. Ni–Mo (III) (13) and Ni–Mo–Si (IV) (14) were prepared by coprecipitation. $NiMoO_4$ was precipitated from a mixed water solution of nickel nitrate and ammonium paramolybdate (concentrations of NiO and MoO_3 were both 80 g/liter) by addition of ammonium hydroxide at pH 6.84 and temperature 80°C. The same technique was used for precipitation of $NiMoO_4$ on the silica support; following Ref. (14) the silica powder was added to the solution of Ni and Mo salts before introducing the precipitation agent. Both bulk and supported $NiMoO_4$ catalysts III and IV were dried at 393 K and calcined in air at 300°C, a procedure which gives the highest hydrogenation activity of the catalyst after sulfidation (13). Co–Mo–HY–Al (V) and Co–Mo–HZSM-5–Al (VI) were prepared by impregnation of a zeolite–alumina support with cobalt nitrate, ammonium paramolybdate in ammonia water solution. The zeolite–alumina support was made by coextrusion of aluminum hydroxide (prepared by a pH oscillating precipitation method from an aqueous solution of aluminum nitrate with ammonium hydroxide (15)) with zeolite powders. All salts were purchased from Fluka. Zeolite HY LZ-Y62 was manufactured by Linde AG and HZSM-5 (CBV-3020) by PQ Corp. The extrudate diameter of catalysts I, II, V, and VI was 1.3–1.5 mm. Coprecipitated powder oxide catalysts III and IV were pelletized by pressing and crushing to a fraction of 0.5–1.0 mm. Before testing, all the catalysts were sulfided by excess of elemental sulfur in hydrogen flow. Elemental sulfur particles (2 g, 20–50 mesh fraction) were loaded in a tubular reactor above a layer of 5 cm^3 of catalyst particles. The reactor was purged with hydrogen at 200 ml/min at room temperature for 0.5 h and then the temperature was increased in three steps, 120–180–240°C, 1 h at every step.

The composition of the catalysts was measured by EDAX (microscope JEM-35, JEOL Co., link system AN-1000, Si–Li detector). The surface area and pore size distribution were measured by BET (ASTM 3663-84) and Hg porosimetry (Amin Co. porosimeter, ASTM 4284-83), respectively. The pore volume including micropores for the oxide catalysts was estimated on the basis of water adsorption at 20°C. The pore volume of peletized sulfide catalysts III and IV was measured on the basis of nitrogen adsorption–desorption isotherms. TEM micrographs were produced on a JEOL Co. microscope 2000-FX, 200 kW.

Preparation of DMDBT and Reaction Solvent

DMDBT was synthesized by alkylation of DBT (Merck, 820409) with dimethylsulfate (Merck, 803071) in the presence of butyl lithium (Aldrich, 109-72-8) at 0°C according to a published method (16). Fractional crystallization with hot methanol was used for DMDBT separation. The product, with a melting point of 151°C, was obtained at about 25% yield.

The solvent nature had a significant effect on the kinetics of DBT HDS because of the competitive adsorption of its components on the catalyst surface (17). Therefore, a model solvent that contained a mixture of paraffinic, naphthenic, and aromatic compounds was prepared. A computer simulation showed that a mixture containing 20% *n*-decane, 50% *n*-octadecane, and 30% tetralin yielded physical properties and boiling point distribution similar to those of gas oil. *n*-Decane and tetralin were purchased from Merck (820383, 809733) and *n*-octadecane from the Humphrey Chem. Co. Inc. (A-18/140/PL). Mixtures were prepared containing 1 wt% DBT or DMDBT, which correspond to 0.17 or 0.15 wt% sulfur, respectively, as normally found in petroleum atmospheric gas oils (3, 4).

Kinetic Measurements

The kinetic measurements were carried out in a high-pressure minipilot plant, automatically controlled and designed for unattended continuous runs. A detailed description of the system, including the hardware and software, is given elsewhere (18). A quantity of 5 g of catalyst mixed with 10 cm^3 silica was loaded into the isothermal zone of the reactor between two layers of 10 cm^3 silica. Prior to performing the kinetic measurements all catalysts were sulfided. The sulfidation procedure included pretreating with elemental sulfur, as described before, then stabilization in the reactor for 24 h with a 2 wt% dimethylsulfide–toluene mixture pumped at LHSV = 3 h^{-1}, 320°C, hydrogen pressure of 5.4 MPa, and hydrogen to liquid ratio 500 Nm^3/m^3. All the kinetic measurements were carried out at 360°C, hydrogen pressure of 5.4 MPa, and hydrogen to liquid ratio 500 Nm^3/m^3. LHSV was varied from 10 to 200 h^{-1}. The liquid product was sampled and analyzed by GC or GC-MS.

Product Analysis

The liquid products were analyzed by GC (Chrompack 9001), equipped with a flame ionization detector and CP-Sil-5 CB capillary column, 10-m long and 0.25-mm i.d. The raw data were processed by the Mosaic GC control software. GC-MS analyses (GC-HP-5890, MSD-5971A) were performed with the HP-1 capillary column (12.5-m long, 0.2-mm i.d.) to identify and quantify by-products.

TABLE 1

Characteristics of Catalysts in Oxide Form

Catalyst	I Co–Mo–Al	II Ni–Mo–Al	III Ni–Mo	IV Ni–Mo–Si	V Co–Mo–HY–Al	VI Co–Mo–H-ZSM-5–Al
Chemical composition, wt%						
CoO	4.2	—	—	—	3.8	4.5
NiO	—	3.4	34.0	30.2	—	—
MoO_3	25.1	24.0	66.0	58.8	20.9	24.8
SiO_2	—	4.1	—	10.1	23.6	32.5
Surface area (m^2/g)	230	140	15	71	308	243
Pore volume (cm^3/g)	0.43	0.30	0.10[a]	0.15[a]	0.52	0.34
Bulk density[a] (g/cm^3)	0.94	0.95	1.30	1.25	0.63	0.58

[a] In sulfide form.

RESULTS

Hydrogenation Route

The potential of the hydrogenation route to enhance the rate of 4,6-DMDBT desulfurization was measured with a set of catalysts that covered an activity range in the hydrogenation of aromatic rings. The composition, surface area, and pore volume of the catalysts (I–IV) in the oxide form are shown in Table 1. Ni–Mo–Al catalysts normally have a higher hydrogenation activity for aromatics than Co–Mo–Al (19). Bulk sulfided $NiMoO_4$ salt is expected to display a higher activity than the alumina-supported Ni–Mo catalysts in aromatics hydrogenation (20, 21), in spite of the fact that its surface area is smaller by an order of magnitude. This is attributed to the inhibition of hydrogenation activity caused by the amphoteric nature of alumina (20). Silica supports, in contrast to alumina, do not reduce the hydrogenation activity of sulfided $NiMoO_4$, thus yielding a more active catalyst as a result of a higher surface area of the active phase (14).

Figure 1 presents the TEM micrographs of Ni–Mo–Si catalyst IV calcined at 300 and 900°C. After calcination at 300°C the unsupported $NiMoO_4$ forms long cylindrical amorphous (13) particles about 100 nm in diameter but within the pores of silica particles this phase could not be identified on the micrograph, probably as a result of its

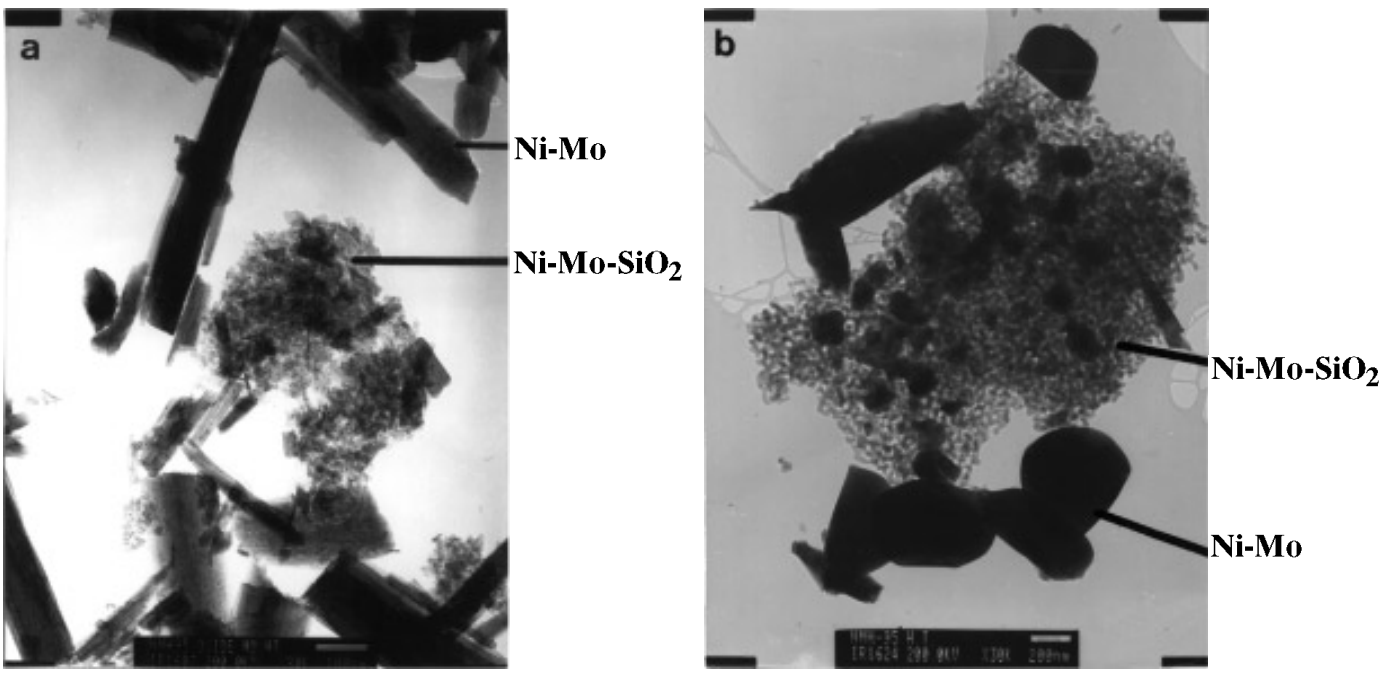

FIG. 1. TEM micrographs of bulk and silica-supported Ni–Mo oxide catalysts calcined at (a) 300°C and (b) 900°C.

very small dimensions. To make it clear we calcined catalyst IV at 900°C. The unsupported $NiMoO_4$ that was stable at this temperature according to XRD data was converted to rounded sintered crystals more than 500 nm in diameter while within the pores of silica particles the same crystals appeared at about 100 nm in diameter. This proves that a part of the $NiMoO_4$ phase in this catalyst calcined at 300°C was indeed encapsulated in pores of the silica support, preventing its sintering at elevated temperatures. Thus it produced a higher surface area of the active component compared to unsupported Ni–Mo catalyst III.

Testing the efficiency of the hydrogenation route in DMDBT HDS considered first the activity of catalysts I–IV in the saturation of aromatic rings. The corresponding tetra- and hexahydro-DBTs are unstable, reacting further in desulfurization reactions. Therefore the desulfurization of DBT and DMDBT yielded two main products in the liquid phase: biphenyl (BPH) and cyclohexylbenzene (CHB), dimethyl-biphenyl (DMBPH) and dimethylcyclohexylbenzene (DMCHB), respectively. The aromatic hydrogenation activity of the catalysts in this particular case could be characterized by the ratio of the conversion to the two products, termed the selectivity parameter α. For all catalysts this selectivity parameter increases with increasing DBT or DMDBT conversion as a result of changing the spacing time as illustrated by the plots in Fig. 2. The effect of conversion on the α values was insignificant compared with the differences in selectivity parameter among the tested catalysts. A comparison of the catalysts at about 80% conversion level (Fig. 2) indicates that the aromatic hydrogenation activity increases significantly from catalyst I to catalyst IV. Furthermore, the α value is higher for DMDBT than for DBT, as a result of higher DMDBT reactivity in aromatic ring hydrogenation, in agreement with results reported by Houalla *et al.* (6).

The rate of sulfur removal was assumed to be pseudo-first-order, as proposed by Houalla *et al.* (6). A semilog plot of the sulfur conversion as a function of the space time in Fig. 3 yielded a good fit of the data. The rate constants calculated from the slope of the plots are listed in Table 2. The rate constants were expressed on the basis of catalyst mass, volume, and surface area to illustrate the intrinsic activity of the catalysts. As expected, the mass or volume rate constants for the Co–Mo–Al catalyst were higher than for Ni–Mo–Al and bulk Ni–Mo catalysts in the HDS of DBT.

The intrinsic activity reflected by the rate constants on a surface basis (k_s) indicates the higher activity of the bulk Ni–Mo catalysts. The rate constants k_w or k_v are normally used for comparison of catalysts in fixed-bed reactors reflecting the differences in %HDS. The HDS activity increased with increasing hydrogenation activity from catalyst II to catalyst IV. The bulk catalysts III and IV were significantly more active than Co–Mo–Al in the case of DMDBT.

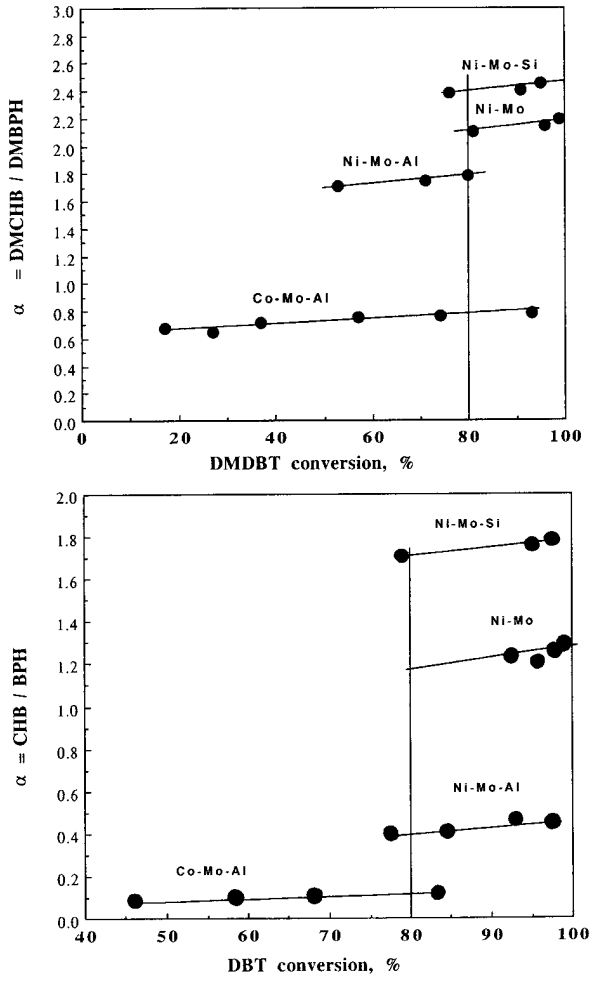

FIG. 2. Effect of DBT and DMDBT conversion with catalysts I–IV on selectivity parameter α.

The ratio of the intrinsic activity of HDS of DMDBT and DBT, represented by the ratio k_{DMDBT}/k_{DBT}, increases sharply with α_{DBT}, representing the relative aromatic hydrogenation activity of the catalysts, as illustrated in Fig. 4. α_{DBT} was estimated from Fig. 2 at 80% conversion. As α_{DBT} reaches a value of about 2, the HDS rates of the two reactants are about the same. This means that the rate of hydrogenation of the aromatic ring in DMDBT preceding the HDS reaction enhanced significantly its HDS rate.

Cracking Route

The efficiency of the cracking activation route in the desulfurization of DMDBT was tested on two Co–Mo–Al catalysts, V and VI, containing zeolites HY and H-ZSM-5. Their composition, surface area, and pore volume are listed in Table 1. The pore volume was higher compared with the basic Co–Mo–Al catalyst due to the pore volume of the zeolites. However, the mesopore volume was reduced, although the pore size distribution did not change as a result

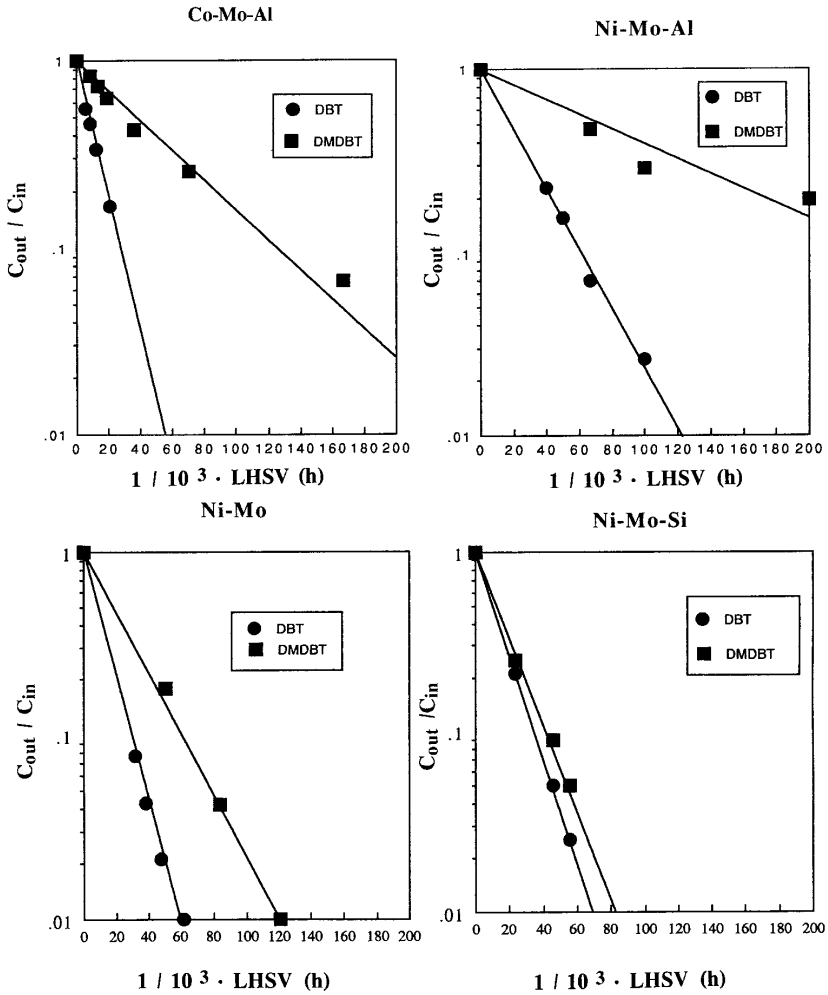

FIG. 3. Pseudo-first-order kinetics of hydrodesulfurization of DBT and DMDBT with catalysts I–IV.

of zeolite introduction, as illustrated in Fig. 5. The kinetic measurements with catalysts V and VI were carried out over a period of 2 h to avoid deactivation (22).

Figure 6 presents the rate constants of DBT and DMDBT HDS calculated for the three catalysts I, V, and VI, assuming first-order reaction. No products other than BPH or DMBPH and CHB or DMCHB were detected with catalyst VI (Co–Mo–HZSM-5–Al). The presence of H-ZSM-5 zeolite increased the HDS rate of DBT by a factor of about 1.5, lowering its α value from 0.15 (catalyst I) to 0.06 (catalyst VI). In contrast, the HDS rate of DMDBT was reduced by a factor of about 1.3 with no significant change in the α value.

TABLE 2

Rate Constants of Hydrodesulfurization of DBT and DMDBT with Catalysts I–IV

Catalyst	Co–Mo–Al	Ni–Mo–Al	Ni–Mo	Ni–Mo–Si
DBT				
k_w, $(cm^3 \cdot g^{-1} \cdot h^{-1})$	96.1	40.3	61.8	55.0
k_v, (h^{-1})	90.4	38.5	80.4	71.5
k_s, $(cm^3 \cdot m^{-2} \cdot h^{-1})$	0.42	0.29	4.1	0.77
DMDBT				
k_w, $(cm^3 \cdot g^{-1} \cdot h^{-1})$	22.1	10.3	30.0	48.1
k_v, (h^{-1})	20.8	9.9	39.1	62.5
k_s, $(cm^3 \cdot m^{-2} \cdot h^{-1})$	0.096	0.073	2.0	0.68

The positive effect of zeolite H-ZSM-5 on the DBT HDS rate could be a result of the direct action of the zeolite strong acidic protons as demonstrated in Refs. (22, 23) for HDS of thiophene with Ni(Co)–Mo–(Ca)–HY catalysts. The lower α value measured with catalyst VI indicates that the H-ZSM-5 zeolite selectively increased the rate of BPH production that proceeded via DBT adsorption on Brønsted acid sites followed by removal of H_2S via β-elimination (24). The negative effect of H-ZSM-5 zeolite on DMDBT HDS could be explained considering the higher molecular dimensions compared with the DBT molecule that led to significantly lower diffusion rates in the zeolite channels.

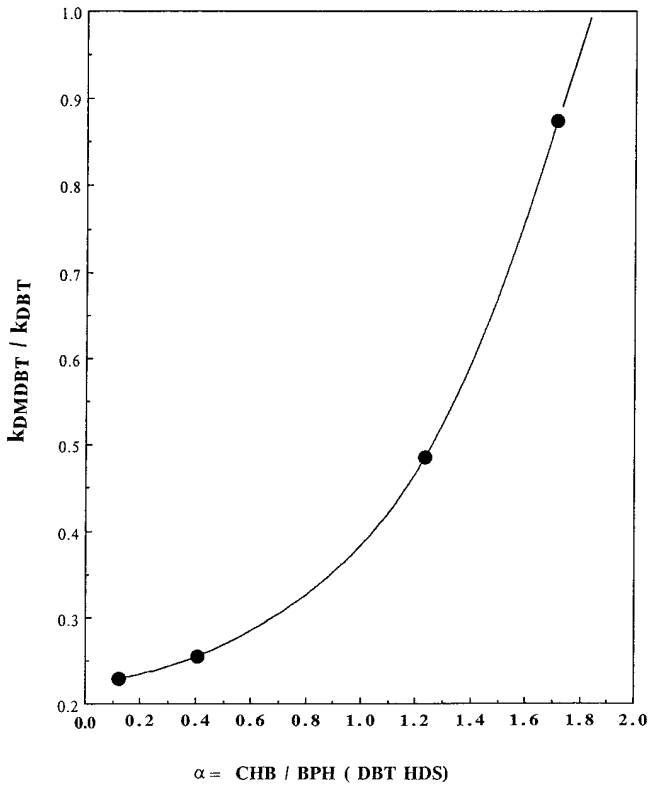

FIG. 4. Correlation between DMDBT/DBT HDS rates ratio and catalysts hydrogenation activity (α_{DBT}).

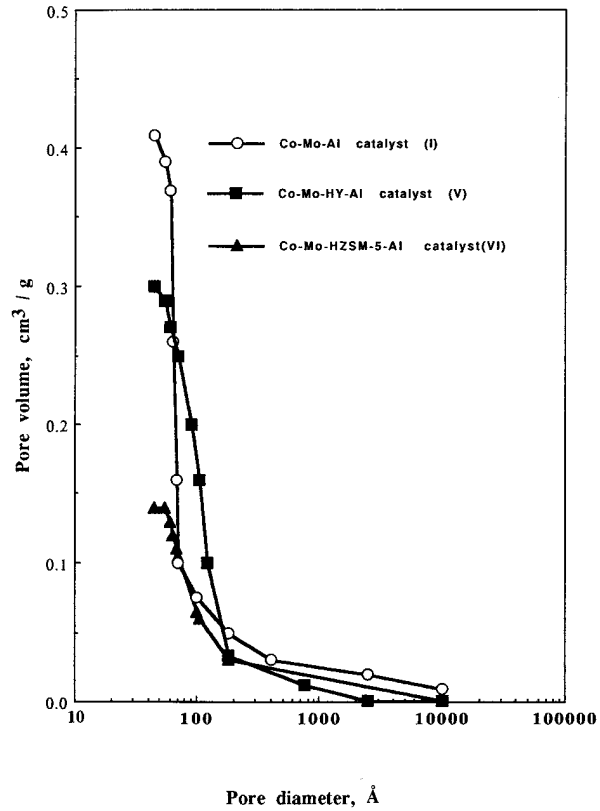

FIG. 5. Pore size distribution in Co–Mo-based catalysts.

Actually, the zeolite component, being inactive in DMDBT HDS, acted as an inert diluent for the active alumina support and thus hindered the formation of Co–Mo–Al–oxide precursors.

Introduction of acidic HY zeolite (catalyst V) increased the HDS rates of both DBT and DMDBT by factors of 1.8 and 3.0, respectively (Fig. 6 The product distribution of DMDBT HDS with catalyst V was different from those obtained with all other catalysts (Table 3, LHSV = 50 h^{-1}). The main product was toluene at about 50% and then benzene at about 20%, both being the result of scission of the C–C bond connecting the benzenic rings in the DMDBT molecule.

The higher HDS rate of DMDBT activated by cracking of the C–C bond in the thiophenic ring compared to demethylation was confirmed by the absence of dimethylphenyl sulfide and diphenyl sulfide in the products, while DMDBT demethylation products (methyldibenzothiophene, tetrahydro-methyl-dibenzothiophene, and tetrahydro-dibenzothiophene) were detected (Table 3). No DMCHB was detected in the DMDBT HDS products obtained with catalyst V as a result of its high reactivity in cracking reactions producing methylcyclohexane and alkyltoluenes. In the case of DBT, substantial scission of the C–C bond connecting the benzenic rings was also observed with

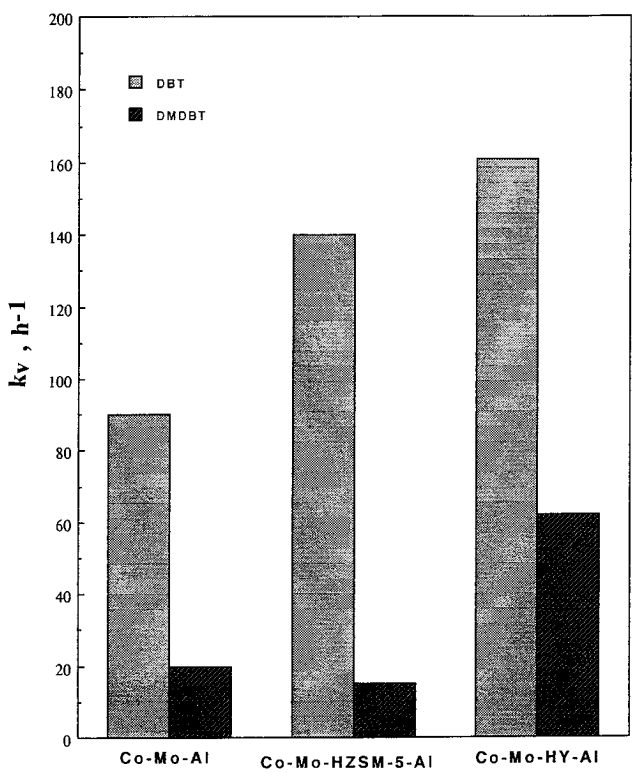

FIG. 6. Effect of zeolite addition on HDS rates of DBT and DMDBT with Co–Mo–Al catalyst.

TABLE 3

DMDBT Conversion Products with Co–Mo–HY–Al Catalyst

Products	wt%
Benzene	19.9
Toluene	47.5
Methylcyclohexane	5.9
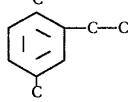 Methylethylbenzene	3.0
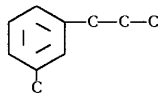 Methylpropylbenzene	8.5
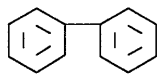 Biphenyl	1.0
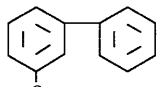 Methylbiphenyl	2.1
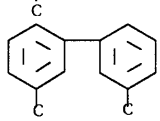 Dimethylbiphenyl	6.5
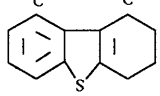 Tetrahydrodibenzothiophene	1.1
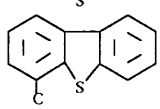 Methyldibenzothiophene	2.7
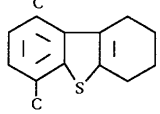 Tetrahydromethyldibenzothiophene	0.3
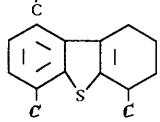 Tetrahydrodimethyldibenzothiophene	0.7

Co–Mo–Al–HY catalyst, producing benzene at about 30% of the products. No CHB was detected in the DBT HDS products obtained with catalyst V as a result of its cracking producing alkylbenzenes.

Figure 7 presents the scheme of DMDBT molecule transformations under HDS conditions with the Co–Mo–Al–HY catalyst. The rate constants shown in Fig. 7 were calculated on the basis of the product mole fractions assuming pseudo-first-order kinetics in all the routes of DMDBT conversion. Intermediates that were not found in DMDBT HDS products are shown in parentheses. Toluene and methylcyclohexane were supposed to be mainly the HDS products of dimethylphenyl sulfide which was not detected as a result of its high reactivity. The Co–Mo–Al catalyst displayed a low activity in DMDBT hydrogenation (Fig. 3), needed for production of those compounds by the second route, through tetrahydro-DMDBT, which was found in the products. This last compound could also give alkyltoluenes as a result of hydrocracking. The same arguments led to the conclusion that benzene was mainly produced as a result of diphenyl sulfide HDS rather than through the second three-stage route (Fig. 7), including a slow hydrogenation step. Comparing the values of the estimated rate constants with the measured overall HDS rate constant for DMDBT showed

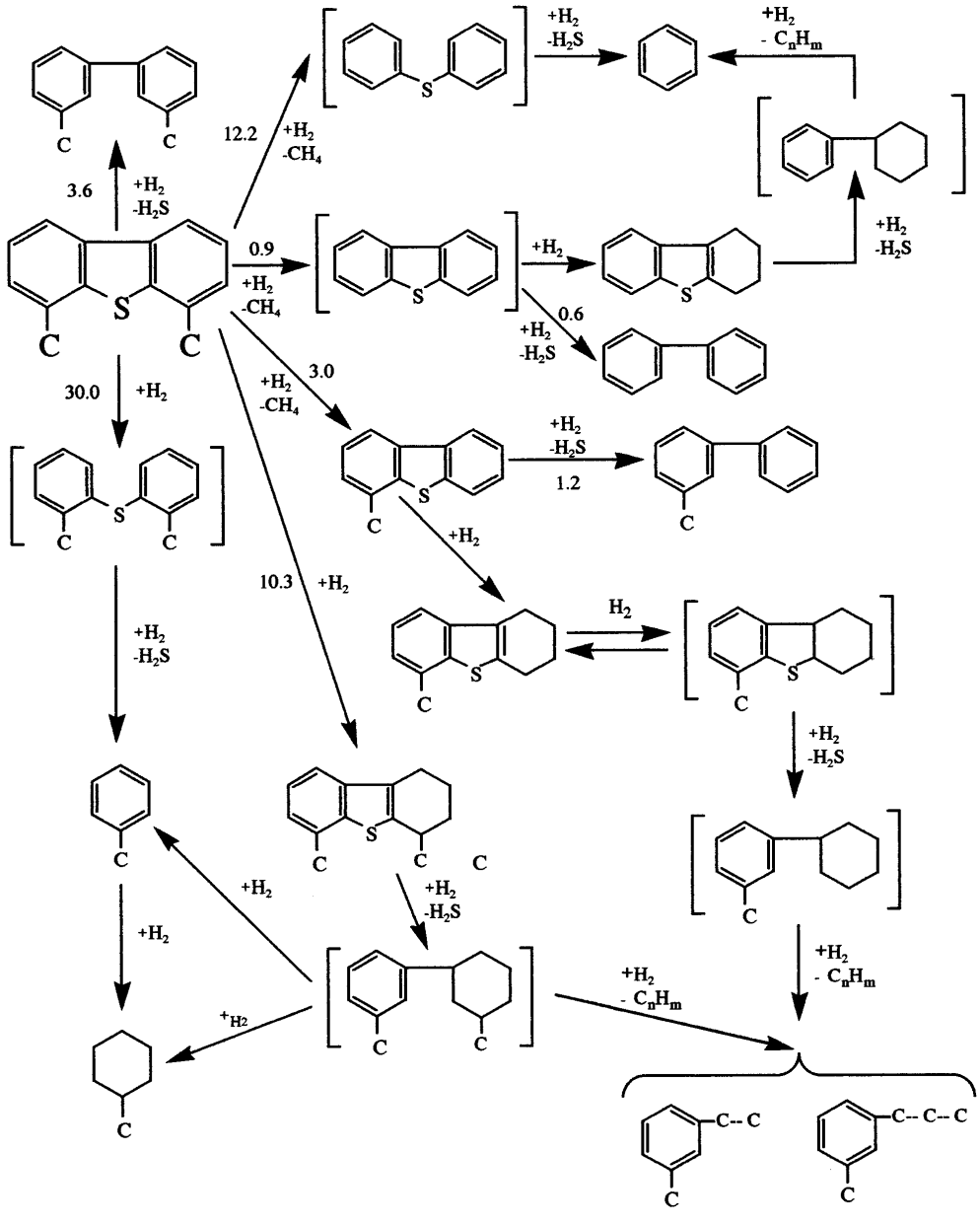

FIG. 7. Conversion of DMDBT in the presence of sulfided Co–Mo–Al–HY catalyst at 360°C, 5.4 MPa, LHSV = 50 h^{-1}: the reaction network. The numbers next to the arrows are pseudo-first-order rate constants (k_v, h^{-1}).

that about 80% of the desulfurized DMDBT was converted through intermediates yielded from "cracking" reactions of which about 70% was converted through scission of the C–C bond connecting the benzenic rings.

DISCUSSION

Increasing the hydrogenation activity of Co(Ni)–Mo sulfide catalysts enhances the HDS rate of DMDBT. The computer simulation of DMDBT configuration (Serena software, PC model PI 89.0) illustrated in Fig. 8 shows that the S atom is screened by methyl groups. The product of DMDBT partial hydrogenation, 4,6-diMe-hexahydro-DBT (HHDMDBT), contains a methyl group, located at an axial position to the cyclohexyl ring, that reduces the steric hindrance at the S–C bond scission making all the atoms in the C–S–C bridge equally accessible to the catalyst surface. Therefore HHDMDBT is expected to be more active than DMDBT in HDS in spite of the presence of the methyl group connected to the second aromatic ring.

The HDS rate of DBT with Ni–Mo catalysts employed in this study, especially Ni–Mo–Al, was lower in compari-

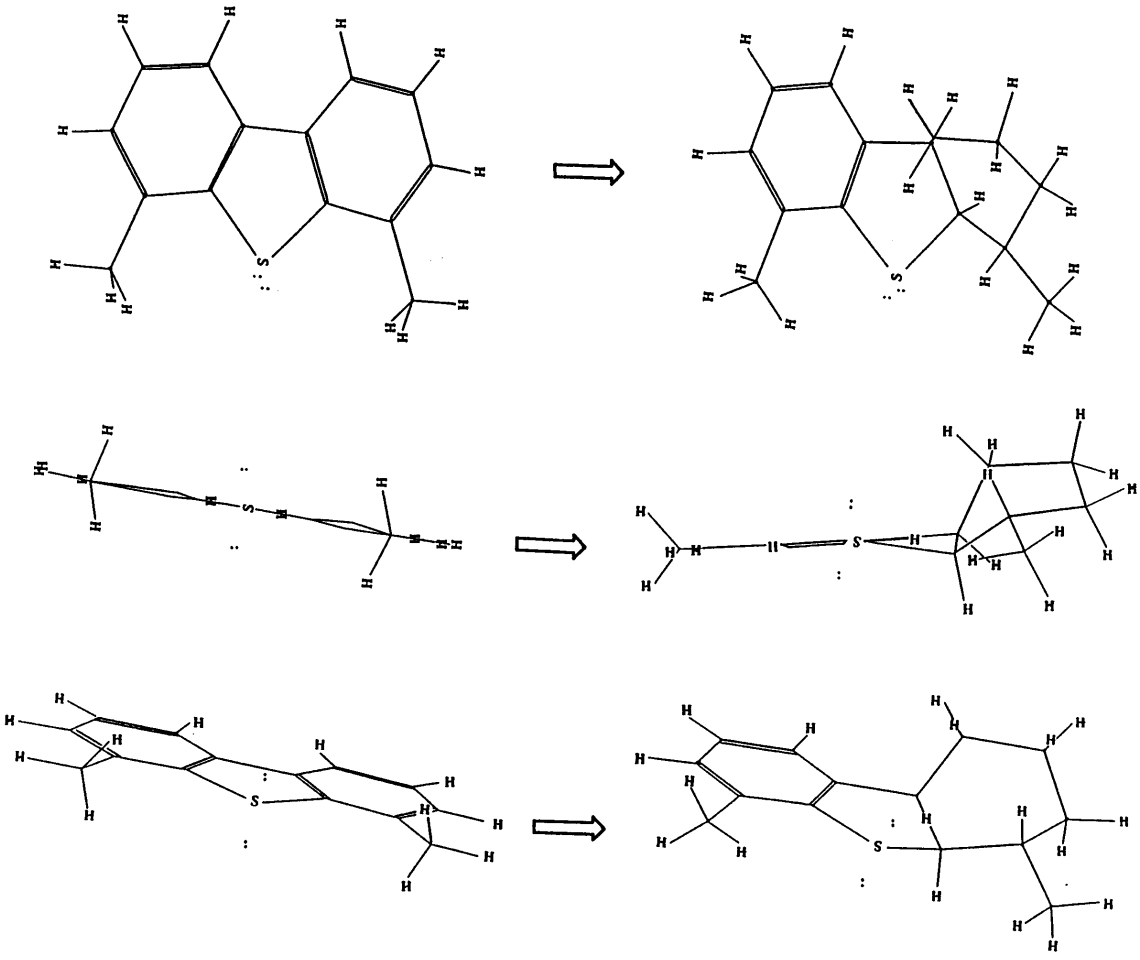

FIG. 8. Computer simulations of the DMDBT molecule structure before and after partial hydrogenation.

son with Co–Mo–Al employed in industrial desulfurization processes (Table 2). Different active sites on the surface of sulfided Co(Ni)–Mo(W) catalysts perform as catalytic centers for aromatic ring saturation and S–C bond scission reactions (21, 25). It appears that an effective catalyst for deep desulfurization of petroleum gas oils has to contain an optimal concentration and ratio of hydrogenation and desulfurization active sites. This would provide effective hydrogenation of aromatic rings in 4,6-DMDBT and other low reactivity substituted dibenzothiophenes as well as effective desulfurization of high reactivity compounds like sulfides, thiophenes, and benzothiophenes. The nature of those active sites is still not well defined (21, 25) rendering the formulation of direct quantitative criteria difficult.

The data obtained in this study provide the basis for the design of an optimal catalyst for deep desulfurization which combines desulfurization activity at the level of commercial Co–Mo–Al catalysts and hydrogenation activity at the level of α for DBT of about 2.

Some published data indicate that hydrogenation and desulfurization active sites are related to different structural elements of sulfide phases on the catalyst surface, namely corners and edges of the $Mo(W)S_2$ crystals (26), bulk Ni–Mo particles and the Ni–Mo–Al monolayer (21, 27), and rim and edge parts of MoS_2 crystal edge planes (28). Optimization of such structures on the catalyst at a proper combination could lead to improved catalysts for deep desulfurization.

This study confirmed the high efficiency of the cracking activation route for desulfurization of DMDBT. Addition of strong acidic components in Co–Mo–Al catalysts enhanced the demethylation the DMDBT and scission of the single C–C bond in the thiophenic ring. Demethylation of DMDBT or scission of the single C–C bond in the thiophenic ring would increase the HDS rate of reaction as a result of removing the screening effect of methyl groups, as illustrated in Fig. 9. In the second case the screening effect would be removed as a result of free rotation of two methyl phenyl groups around the C–S–C bridge. The preparation of HDS catalysts which contain acid sites could be a solution to deep desulfurization. However, zeolite catalysts are deactivated at a high rate as a result of coking (22) and

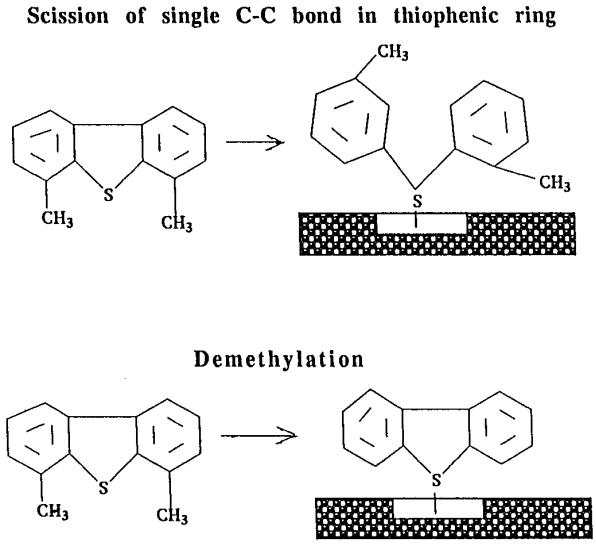

FIG. 9. DMDBT molecule "activation" according to cracking routes.

poisoning with nitrogen compounds present in petroleum gas oils (29). The published data evident for positive zeolite effects on Co(Ni)–Mo–Al catalysts HDS efficiency (22, 30, 31, 32) were measured in short runs with model compounds in absence of nitrogen. Zeolite deactivation in long runs with petroleum gas oils containing nitrogen compounds could be a detrimental factor in the implementation of such solutions to desulfurization catalysts. The high efficiency of the cracking activation route in deep HDS should support further work to resolve potential deactivation problems.

ACKNOWLEDGMENTS

The authors thank Mrs. Y. Press for catalyst preparation, Dr. R. Rachman for assistance with kinetic measurements, Dr. L. Kogan for conducting the GC-MS analysis, and Dr. I. Levy for conducting the TEM analysis.

REFERENCES

1. Unzelman, G. H., *Oil Gas J.* June **19**, 55 (1987).
2. Takatsuka, T., Wada, Y., Suzuki, H., Komatsu, S., and Morimura, Y., *J. Jpn. Pet. Inst.* **35**, 179 (1992).
3. Kabe, T., Ishihara, A., and Tajima, H., *Ind. Eng. Chem. Res.* **31**, 1577 (1992).
4. Amorelli, A., Amos, Y. D., Haisig, C. P., Koaman, J. J., Jonker, R. J., de Wind, M., and Vrieling, J., *Hydrocarbon Proc.* June, 93 (1992).
5. Ishihara, A., Tajima, H., and Kabe, T., *Chem. Lett.* 669 (1992).
6. Houalla, M., Broderic, D. H., Sapre, A. V., Nag, N. K., de Beer, V. H. J., Gates, B. C., and Kwart, H., *J. Catal.* **61**, 523 (1980).
7. Ma, X., Sakanishi, K., and Mochida, I., *Ind. Eng. Chem. Res.* **33**, 218 (1994).
8. Ma, X., Sakanishi, K., Isoda, T., and Mochida, I., *Ind. Eng. Chem. Res.* **34**, 748 (1995).
9. Kabe, T., Ishihara, A., and Zhang, Q., *Appl. Catal. A* **97**, L1 (1993).
10. Lamure-Meille, V., Schulz, E., Lemaire, M., and Vrinat, M., *Appl. Catal.* **131**, 143 (1995).
11. Takaaki, I., Xiaoliang, X., and Isao, M., *Sekiyu Gakkaishi* **37**, 368 (1994).
12. Rollmann, L. D., Howley, P. A., Mazzone, D. N., and Timken, H. K. C., AIChE 1994 Spring National Meeting, Atlanta, April 17–21, 1994, Paper No. 53d.
13. Landau, M. V., Alexeenko, L. N., Vinogradova, O. V., Michailov, V. I., and Nefedov, B. K., *Kinet. Katal.* **30**, 933 (1989). [Russian]
14. Landau, M. V., Alexeenko, L. N., Nikulina, L. I., Vinogradova, O. V., Nefedov, B. K., Konovalchikov, L. D., Stein, V. I., and Podobaeva, T. P., *Chem. Technol. Fuels Oils* **N1**, 11 (1991). [Russian]
15. Wakabayashi, M., Ono, T., Togari, O., and Nakamura, M., Ger. Offen. 29326448, 1980 (CA 92P: 170026e).
16. Gerdil, R., and Lucken, E., A., *J. Am. Chem. Soc.* **87**, 213 (1965).
17. Ishihara, A., Itoh, T., Hino, T., Nomura, M., Qi, P., and Kabe, T., *J. Catal.* **140**, 184 (1993).
18. Herskowitz, M., Landau, M. V., Harel, A., and Cohen, B., submitted for publication.
19. Stanislaus, A., and Cooper, B. H., *Catal. Rev.-Sci. Eng.* **36**, 75 (1994).
20. Landau, M. V., Alexeenko, L. N., Nefedov, B. K., Kipnis, M. A., Agievsky, D. A., Chukin, G. D., Sergienko, S. A., and Kvashonkin, V. I., *Kinet. Katal.* **25**, 934 (1984). [Russian]
21. Landau, M. V., Michailov, V. I., Tsisun, E. L., Samgina, T. Yu., Chukin, G. D., Vinigradova, O. V., Nefedov, B. K., and Slinkin, A.A., *Kinet. Katal.* **27**, 931 (1986). [Russian]
22. Welters, W. J. J., de Beer, V. H. J., and van Santen, R. A., *Appl. Catal. A* **119**, 253 (1994).
23. Welters, W. J. J., Vorbeck, G., Zandbergen, H. W., de Haan, J. W., de Beer, V. H. J., and van Santen, R. A., *J. Catal.* **150**, 155 (1994).
24. Kolboe, S., *Can. J. Chem.* **47**, 352 (1969).
25. Chianelli, R. R., and Daage, M., *Adv. Catal.* **40**, 177 (1994).
26. Moreau, C., and Geneste, P., *in* "Theoretical Aspects of Heterogeneous Catalysis" (J. B. Moffat, Ed.), p. 256. Van Nostrand–Reinhold, New York, 1990.
27. Landau, M. V., Alexeenko, L. N., Nefedov, B. K., Chukin, G. D., Agievsky, D. A., Kvashonkin, V. I., Michailov, V. I., Surin, S. A., and Pavlova, L. I., *Kinet. Katal.* **27**, 440 (1986). [Russian]
28. Daage, M., and Chianelli, R. R., *J. Catal.* **149**, 414 (1994).
29. Nat, P. J., *Erdol Kohle Erdgas Petrochem.* **42**, 447 (1989).
30. Visotsky, A. V., Chuikova, N. A., and Lipovich, V. G., *Kinet. Katal.* **18**, 1345 (1977). [Russian]
31. Surin, S. A., Aliev, R. R., and Nefedov, B. K., *Petrol. Chem. USSR* **21**, 385 (1981). [Russian]
32. Welters, W. J. J., Koranyi, T. I., de Beer, V. H. J., and van Santen, R. A., *in* "New Frontiers in Catalysis" (L. Guczi, F. Solymosi, and P. Tétényi, Eds.), p. 1931. Elsevier, Amsterdam, 1992.